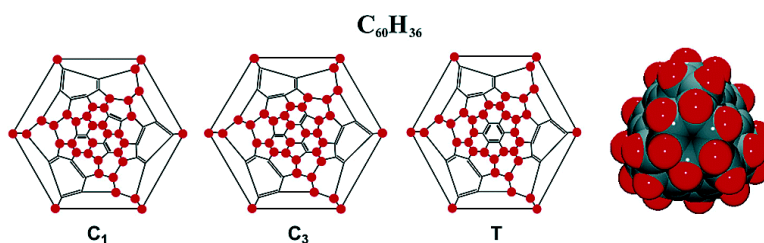


## Thermodynamic Rearrangement Synthesis and NMR Structures of $C_1$ , $C_3$ , and $T$ Isomers of $C_60H_{36}$

Andrei A. Gakh, Andrew Yu. Romanovich, and Ad Bax

*J. Am. Chem. Soc.*, **2003**, 125 (26), 7902-7906 • DOI: 10.1021/ja035332t • Publication Date (Web): 06 June 2003

Downloaded from <http://pubs.acs.org> on March 29, 2009



### More About This Article

Additional resources and features associated with this article are available within the HTML version:

- Supporting Information
- Links to the 3 articles that cite this article, as of the time of this article download
- Access to high resolution figures
- Links to articles and content related to this article
- Copyright permission to reproduce figures and/or text from this article

[View the Full Text HTML](#)



## Thermodynamic Rearrangement Synthesis and NMR Structures of $C_1$ , $C_3$ , and $T$ Isomers of $C_{60}H_{36}$

Andrei A. Gakh,<sup>\*,†</sup> Andrew Yu. Romanovich,<sup>†</sup> and Ad Bax<sup>‡</sup>

Contribution from the Oak Ridge National Laboratory, Oak Ridge, Tennessee 37831, and Laboratory of Chemical Physics, NIDDK, National Institutes of Health, Bethesda, Maryland 20892

Received March 26, 2003; E-mail: gakhaa@ornl.gov

**Abstract:** The structures of three  $C_{60}H_{36}$  isomers, produced by high-temperature transfer hydrogenation of  $C_{60}$  in a 9,10-dihydroanthracene melt, was accomplished by 2D  $^1H$ -detected NMR experiments, recorded at 800 MHz. The unsymmetrical  $C_1$  isomer is found to be the most abundant one (60–70%), followed by the  $C_3$  isomer (25–30%) and the least abundant  $T$  isomer (2–5%). All three isomers are closely related in structure and have three vicinal hydrogens located on each of the 12 pentagons. Facile hydrogen migration on the fullerene surface during annealing at elevated temperatures is believed to be responsible for the preferential formation of these thermodynamically most stable  $C_{60}H_{36}$  isomers. This hypothesis was further supported by thermal conversion of  $C_{60}H_{36}$  isomers to a single  $C_{3v}$  isomer of  $C_{60}H_{18}$ .

### Introduction

$C_{60}H_{36}$  was one of the first derivatives of  $C_{60}$  ever made,<sup>1</sup> and it appears to be the ultimate hydrogenation product under various hydrogenation conditions.<sup>2,3</sup> This and other hydrofullerenes are of particular interest as models for the investigation of surface hydrogenation–dehydrogenation processes in carbon nanosystems. Fully surface-hydrogenated carbon nanomaterials can reach hydrogen capacity as high as 7.7% for  $CH_{1.0}$  composition, thus exceeding the 6.5% hydrogen storage systems requirement.<sup>3,4</sup>

Despite its easy availability and prodigious interest,  $C_{60}H_{36}$  has defied numerous attempts to determine its structure for almost 10 years. Selected bibliographic materials with 67 references pertaining to the history of  $C_{60}H_{36}$  research are included as Supporting Information. Here, we report the results of our NMR structure determination of the three predominant  $C_{60}H_{36}$  isomers, consistently produced by high-temperature hydrogenation of  $C_{60}$ , which provide compelling evidence for facile hydrogen migration on the fullerene surface at high temperatures.

### Results and Discussion

Hydrogenation of  $C_{60}$  to  $C_{60}H_{36}$  can be performed by several methods, including Birch hydrogenation, catalytic hydrogenation, Zn-alloy reduction in HCl, and radical transfer hydrogenation.<sup>3,4</sup>

A recent report indicated that low-temperature hydrogenation (Birch conditions) affords a complex mixture of isomers, whereas high-temperature transfer hydrogenation in a 9,10-dihydroanthracene melt at 350 °C yields mainly two isomers of  $C_{60}H_{36}$  ( $C_1$  and  $C_3$ ), in roughly a 3:1 ratio.<sup>5</sup> Because of this apparent isomer selectivity, we chose this method to generate material for structural exploration.

**Synthesis.** High-temperature hydrogenation of  $C_{60}H_{36}$  was performed as described earlier,<sup>5,6</sup> but with some minor modifications. The reported procedure<sup>5</sup> involved HPLC purification of the products. To avoid potential loss and/or isomerization of  $C_{60}H_{36}$  isomers during HPLC separation, we investigated this reaction in an attempt to find conditions at which  $C_{60}H_{36}$  samples can be obtained with satisfactory purity for NMR analysis without requiring chromatographic separation. The major factors influencing the production of high-quality  $C_{60}H_{36}$  samples were found to be time and temperature. Longer reaction time (1.5 h compared to 0.75 h at 350 °C)<sup>5</sup> favored isomer selectivity (annealing process, see below). Unfortunately, it also promoted subsequent dehydrogenation of  $C_{60}H_{36}$  isomers to  $C_{3v}$   $C_{60}H_{18}$ .<sup>6,7</sup> The best results were achieved when the reaction was carried out at slightly lower temperature,  $340 \pm 10$  °C, for a total duration of 2 h. The  $C_{60}H_{36}$  samples had satisfactory stability in the solution (4–6 h), even in the presence of a small amount of oxygen. They also had reasonable solubility in  $CDCl_3$  (5–7 g/L), thus eliminating the need of toxic  $CS_2$  as a cosolvent.

**Structure Determination.** The very limited spectral dispersion in both the  $^1H$  and  $^{13}C$  spectra of the mixture of  $C_{60}H_{36}$

<sup>†</sup> Oak Ridge National Laboratory.

<sup>‡</sup> National Institutes of Health.

- (1) Hauffler, R. E.; Conceicao, J.; Chibante, L. P. F.; Chai, Y.; Byrne, N. E.; Flanagan, S.; Haley, M. M.; O'Brien, S. C.; Pan, C.; Xiao, Z.; Billups, W. E.; Ciufolini, M. A.; Hauge, R. H.; Margrave, J. L.; Wilson, L. J.; Curl, R. F.; Smalley, R. E. *J. Phys. Chem.* **1990**, *94*, 8634–8636.
- (2) Nossal, J.; Saini, R. K.; Alemany, L. B.; Meier, M.; Billups, W. E. *Eur. J. Org. Chem.* **2001**, 4167–4180.
- (3) Tarasov, B. P.; Goldshleger, N. F.; Moravskii, A. P. *Usp. Khim.* **2001**, *70*, 149–166.
- (4) Dillion, A. C.; Heben, M. J. *Appl. Phys. A* **2001**, *72*, 133–142.

- (5) Nossal, J.; Saini, R. K.; Sadana, A. K.; Bettinger, H. F.; Alemany, L. B.; Scuseria, G. E.; Billups, W. E.; Saunders, M.; Khong, A.; Weisemann, R. *J. Am. Chem. Soc.* **2001**, *123*, 8482–8495.
- (6) Rüdhardt, C.; Gerst, M.; Ebenhoch, J.; Beckhaus, H.-D.; Campbell, E. E. B.; Tellmann, R.; Schwarz, H.; Weiske, T.; Pitter, S. *Angew. Chem., Int. Ed. Engl.* **1993**, *32*, 584–586.
- (7) Darvish, A. D.; Avent, A. G.; Taylor, R.; Walton, D. R. M. *J. Chem. Soc., Perkin Trans. 2* **1996**, 2051–2054.

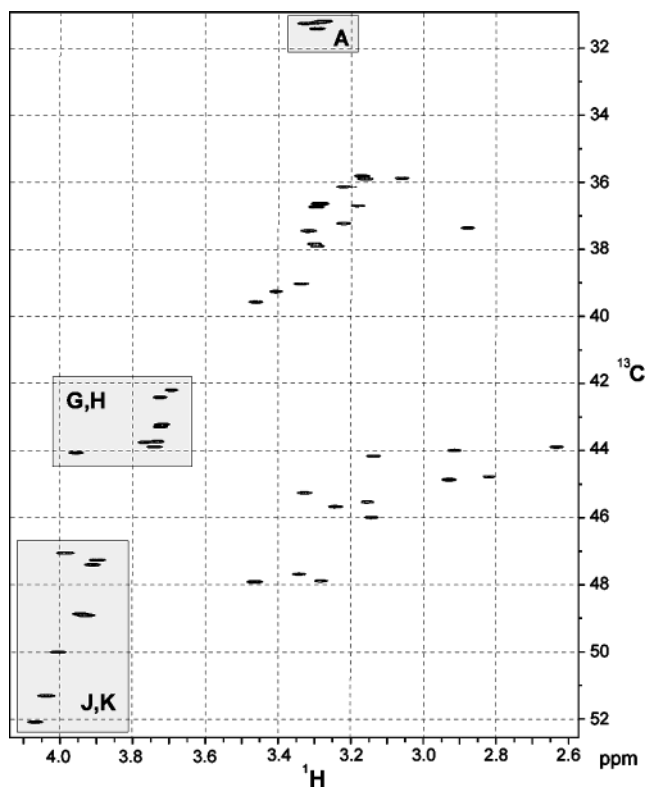


**Figure 1.** The 800-MHz HSQC spectrum of  $C_1$ ,  $C_3$ , and  $T$   $C_{60}H_{36}$  mixture.

isomers required both the highest available magnetic field strength and special adaptation of the inverse detected NMR experiments, to obtain sufficient resolution in the inverse detected  $^1H$ - $^{13}C$  correlation spectra. Because of the long  $^{13}C$  transverse relaxation times of  $C_{60}H_{36}$  resonances in  $CDCl_3$  ( $> 100$  ms), a very large number of increments could be sampled in this dimension without loss of sensitivity per unit of measuring time.<sup>8</sup> This resulted in excellent resolution in the  $^{13}C$  dimension, with line widths of about 0.03 ppm. Only three 2D NMR spectra were utilized for the structure determination process:  $^1H$ - $^{13}C$  HSQC<sup>9</sup> for identifying the one-bond correlations (Figure 1),  $^1H$ - $^{13}C$  COSY-HSQC<sup>10</sup> for connecting  $^{13}C$  resonances to protons two-bonds removed, and  $^1H$ - $^{13}C$  TOCSY-HSQC<sup>10</sup> for resolving ambiguities in the analysis of the  $^1H$ - $^{13}C$  COSY-HSQC spectrum. The high resolution obtained in the  $^{13}C$  dimension was critical for minimizing overlap, particularly in the relayed 2D spectra.

$^{13}C$  and  $^1H$  spectral data of  $C_{60}H_{36}$  samples (CH fragments) are presented in Table 1 and are in general agreement with the previously reported data.<sup>5</sup> The spectra have 36 signals of CH fragments assigned to a  $C_1$  isomer (60–70%), 12 signals assigned to a  $C_3$  isomer (25–30%), and three additional signals with lower intensity which we assigned to a  $T$  isomer (2–5%) of  $C_{60}H_{36}$ . The assignment of these  $^{13}C$  peak sets was made based on the results of the COSY-HSQC and TOCSY-HSQC experiments and was further confirmed by evaluation of peak heights (cf. A4, A3, A2 with A1; H25 with H24; G22 with G23; K43 with K44, Figure 2).<sup>11</sup>

Structure elucidation of the unsymmetrical  $C_1$  isomer of  $C_{60}H_{36}$  is a formidable task, taking into account the possibility

**Table 1.**  $^{13}C$  and  $^1H$  Chemical Shifts of the Three  $C_{60}H_{36}$  Isomers in  $CDCl_3$

| signal                         | $\delta$ ( $^{13}C$ ) <sup>a</sup> | $\delta$ ( $^1H$ ) <sup>a</sup> | signal | $\delta$ ( $^{13}C$ ) <sup>a</sup> | $\delta$ ( $^1H$ ) <sup>a</sup> |
|--------------------------------|------------------------------------|---------------------------------|--------|------------------------------------|---------------------------------|
| <b><math>C_1</math> Isomer</b> |                                    |                                 |        |                                    |                                 |
| A2                             | 31.34                              | 3.28                            | G22    | 43.32                              | 3.72                            |
| A3                             | 31.37                              | 3.32                            | G29    | 44.17                              | 3.96                            |
| A4                             | 31.52                              | 3.29                            | H21    | 42.52                              | 3.73                            |
| B40                            | 47.79                              | 3.34                            | H25    | 43.85                              | 3.77                            |
| B41                            | 47.99                              | 3.29                            | H26    | 43.99                              | 3.74                            |
| C14                            | 37.94                              | 3.30                            | I30    | 44.27                              | 3.14                            |
| C15                            | 38.01                              | 3.29                            | 31     | 44.89                              | 2.82                            |
| C18                            | 39.36                              | 3.41                            | I34    | 45.64                              | 3.16                            |
| D16                            | 37.47                              | 2.88                            | I36    | 46.10                              | 3.15                            |
| D27                            | 44.00                              | 2.63                            | J37    | 47.16                              | 3.99                            |
| D28                            | 44.10                              | 2.92                            | J45    | 50.11                              | 4.01                            |
| E6                             | 35.98                              | 3.06                            | J47    | 52.20                              | 4.07                            |
| E10                            | 36.81                              | 3.18                            | K38    | 47.37                              | 3.89                            |
| E19                            | 39.67                              | 3.46                            | K39    | 47.51                              | 3.91                            |
| F7                             | 36.00                              | 3.16                            | K43    | 49.01                              | 3.93                            |
| F9a                            | 36.74                              | 3.29                            | L8     | 36.25                              | 3.22                            |
| F11                            | 36.84                              | 3.30                            | L17    | 39.13                              | 3.34                            |
| G20                            | 42.30                              | 3.69                            | L33    | 45.36                              | 3.33                            |
| <b><math>C_3</math> Isomer</b> |                                    |                                 |        |                                    |                                 |
| A1                             | 31.31                              | 3.27                            | G23    | 43.39                              | 3.73                            |
| B42                            | 48.02                              | 3.47                            | H24    | 43.83                              | 3.73                            |
| C13                            | 37.56                              | 3.32                            | I35    | 45.78                              | 3.24                            |
| D32                            | 44.97                              | 2.93                            | J46    | 51.42                              | 4.04                            |
| E12                            | 37.33                              | 3.22                            | K44    | 49.02                              | 3.92                            |
| F5                             | 35.92                              | 3.17                            | L9b    | 36.75                              | 3.29                            |
| <b><math>T</math> Isomer</b>   |                                    |                                 |        |                                    |                                 |
| A                              | 31.37                              | 3.19                            |        |                                    |                                 |
| H                              | 43.61                              | 3.67                            |        |                                    |                                 |
| K                              | 49.25                              | 3.86                            |        |                                    |                                 |

<sup>a</sup> NMR data are presented in ppm versus internal reference [ $CDCl_3$  at  $\delta$  77.23 ppm ( $^{13}C$ ) and 7.24 ( $^1H$ )].

of more than 600 trillion solutions.<sup>12</sup> The key to solving the structure was the identification of six CH groups interconnected in a six-member ring. Only one such combination was found: A2-K39-A3-K38-A4-K43 (Figure 3). There exists only one possible placement for this ring in the  $C_{60}$  framework (Figure 4a). The discovery of this key fragment allows for step-by-step structure solution (see detailed discussion in the Supporting Information).

Unique assignment of all 36 CH groups in the structure of the  $C_1$  isomer of  $C_{60}H_{36}$  provided an opportunity for 2D area analysis ( $^{13}C$ ,  $^1H$ ) of their NMR signals. Several compact groups of signals were identified (Figure 1). Type A signals (A2, A3, A4) were in a very narrow range of 31.3–31.6/3.27–3.32 ppm  $^{13}C$ / $^1H$ . Other compact groups of signals were J/K types in the 47.1–52.2/3.89–4.07 ppm region and G/H types, all located within the narrow range of 42.2–44.2/3.69–3.96 ppm.

Structure analysis of the  $C_3$  isomer is initiated by identification of the signals of three identical CHCHCHCH(CH)<sub>2</sub> fragments as A1-K44-H24-G23-J46(C13,F5) in the COSY-HSQC spectrum. Due to the  $C_3$  symmetry, there is only one possible placement of these three fragments in the  $C_{60}$  framework (Figure 4b). A detailed description of  $C_3$  structure elucidation is included as Supporting Information.

(11) In our  $C_{60}H_{36}$  samples the  $C_3/C_1$  ratio was slightly higher than the exact 1/3 ratio reported previously.<sup>5</sup> As a result,  $C_3$  signals (magnified three times compared to  $C_1$  signals due to the symmetry) were about 10–20% higher than the corresponding  $C_1$  signals. The  $T$  isomer signal set was identified on the basis of its high symmetry, but lower relative abundance (2–5%), which translates to about half the relative intensity compared to signals of the  $C_1$  isomer (see Figure 2). Smaller signal intensities of the  $T$  isomer have been observed in the  $CDCl_3$  saturated solutions used for recording the 2D NMR spectra. Reference spectra of  $C_1/C_3$  mixtures without the  $T$  isomer were reported elsewhere.<sup>5</sup>

(12) Balasubramanian, K. *Chem. Phys. Lett.* **1991**, *182*, 257–262.

(8) Levitt, M. H.; Bodenhausen, G.; Ernst, R. R. *J. Magn. Reson.* **1984**, *58* (3), 462–472.

(9) Bodenhausen, G.; Ruben, D. J. *Chem. Phys. Lett.* **1980**, *69*, 185–189.

(10) Lerner, L.; Bax, A. *Carbohydr. Res.* **1987**, *166*, 35–46.

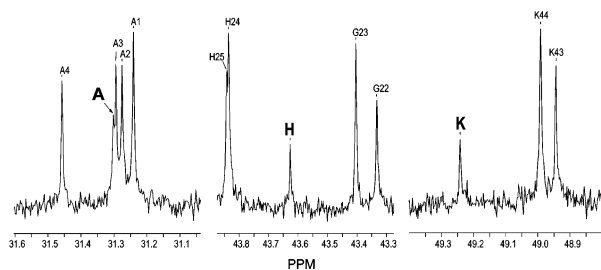


**Figure 2.**  $^{13}\text{C}$  spectra showing three peaks (A, H, K) of the *T* isomer of  $\text{C}_{60}\text{H}_{36}$ .

Structure determination of the elusive<sup>5</sup> *T* isomer of  $\text{C}_{60}\text{H}_{36}$  was made by using the results of 2D NMR experiments and computer analysis (see the Supporting Information). Final selection was made by calculation of relative thermodynamic stabilities of the only two candidates compatible with the NMR data (a second *T* isomer is almost 50 kcal/mol less thermodynamically stable than the selected one, Figure 4c). Similar computational results have been reported previously.<sup>13</sup>

**Surface Hydrogenation.** Determination of the structures of all three  $\text{C}_{60}\text{H}_{36}$  isomers (together comprising over 80% of the  $\text{C}_{60}\text{H}_{36}$  samples) provides additional insight into the nature of surface hydrogenation of the fullerene  $\text{C}_{60}$  and the structure of these hydrides.

First, all three isomers are closely related in structure as well as in their “tetrahedral” 3D appearance (Figure 4d). The most abundant  $C_1$  isomer and less abundant  $C_3$  isomer differ only by the position of one isolated double bond, which has little effect on the overall geometry of the molecule. In the minor *T* isomer, three out of four benzene fragments are positioned identically to both  $C_1$  and  $C_3$  isomers.

It is also notable that in all three isomers, pentagons have exactly three vicinal hydrogen atoms attached. This explains the “magic” substitution number (36): the original  $\text{C}_{60}$  structure contains 12 pentagons. The underlying reasons for this behavior are not clear at this time, but thermodynamic considerations must play a major role. Computer calculations showed that displacement of one isolated double bond to a hexagon–hexagon junction from a pentagon–hexagon juncture results in a substantial energy loss.<sup>13</sup> While it is premature to conclude that all  $\text{C}_{60}\text{H}_{36}$  isomers would adopt this rule, thus far all known structures of  $\text{C}_{60}\text{X}_{36-48}$  ( $X = \text{H}, \text{F}$ ) seem to obey it.<sup>14–16</sup>

Computational modeling demonstrated another strong link between the three  $\text{C}_{60}\text{H}_{36}$  isomers reported here: they all belong to a set of the thermodynamically most stable structures.<sup>5,13</sup> Unfortunately, the precision of existing computational methods does not allow for a clear distinction between  $\text{C}_{60}\text{H}_{36}$  isomers (the differences in thermodynamic stability were typically less than 0.2 kcal/bond and therefore statistically indistinguishable).<sup>5</sup> Nevertheless, certain trends are clear from the analysis of these data.

The average calculated thermodynamic stabilities of the *T*,  $C_3$ , and  $C_1$  isomers rank as follows:  $T \sim C_3 > C_1$ .<sup>5,13</sup> The actual

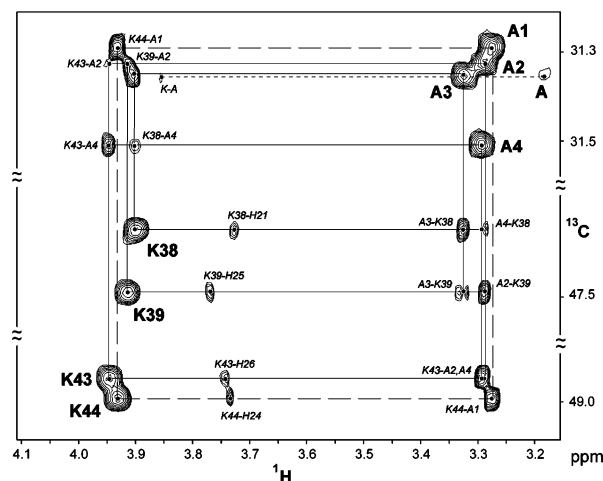


**Figure 3.** Composite region of the COSY-HSQC spectrum, showing the key connectivities for the six-membered protonated ring of the  $C_1$  isomer (solid lines), the  $C_3$  isomer (long dashes), and the *T* isomer (short dashes). One-bond  $^1\text{H}$ – $^{13}\text{C}$  connectivities are marked in regular font. Cross-peaks are marked in italic type. The spectrum has been phased so that the diagonal peaks (one-bond connectivities) are absorptive, and cross-peaks (two-bond connectivities) are antiphase dispersive in the  $^1\text{H}$  dimension. Only positive contours are shown.

distribution of these isomers in  $\text{C}_{60}\text{H}_{36}$  samples is almost reversed:  $C_1 > C_3 \gg T$ . Although the existence of residual kinetic factors cannot be ruled out,<sup>17</sup> the experimental data regarding high-temperature hydrogenation of  $\text{C}_{60}$  argue against this possibility. A plausible explanation of this reverse distribution pattern involves consideration of the entropy component in the Gibb’s free energy equation which governs the equilibrated processes:  $\Delta G = \Delta H - T\Delta S$ . The entropy factor would favor the formation of the least symmetrical isomers (other factors being equal), which is in agreement with the experimental data.

The computer modeling studies also provided some additional insight regarding the observed stoichiometric selectivity of the hydrogenation process. As mentioned earlier,  $\text{C}_{60}\text{H}_{36}$  is the ultimate product of many hydrogenation reactions. Computations showed that less hydrogenated molecules, such as  $\text{C}_{60}\text{H}_{34}$ , typically have less (or about the same) strain energy compared to that of  $\text{C}_{60}\text{H}_{36}$ . At the same time, more hydrogenated molecules, such as  $\text{C}_{60}\text{H}_{38}$  and higher, are significantly more strained. The likely reason for this is unfavorable hydrogen–hydrogen interactions in highly hydrogenated pentagons. Structural constraints dictate that starting with  $\text{C}_{60}\text{H}_{38}$  all hydro[60]-fullerenes contain five-membered rings with at least four hydrogen atoms. Similar computational results were reported for  $\text{C}_{70}\text{H}_{36}$ , suggesting the general nature of these observations.<sup>18</sup>

**Hydrogen Rearrangement.** Available experimental data (primarily improvement in isomer selectivity by applying “annealing” for the preparation of  $\text{C}_{60}\text{H}_{36}$ , as well as thermodynamic properties of thus produced isomers) point to the

- (13) Clare, B. W.; Kepert, D. L. *J. Mol. Struct.* **1999**, *466*, 177–186. Clare, B. W.; Kepert, D. L. *J. Mol. Struct.* **2002**, *589*, 195–207.  
 (14) Gakh, A. A.; Tuinman, A. A.; Adcock, J. L.; Sachleben, R. A.; Compton, R. N. *J. Am. Chem. Soc.* **1994**, *116*, 819–820.  
 (15) Gakh, A. A.; Tuinman, A. A. *Tetrahedron Lett.* **2001**, *42* (41), 7133–7135.  
 (16) Avent, A. G.; Clare, B. W.; Hitchcock, P. B.; Kepert, D. L.; Taylor, R. *Chem. Commun.* **2002**, (20), 2370–2371.

- (17) An alternative explanation of the “reverse” distribution of isomers entails slow kinetics of the interconversion of  $C_1$ ,  $C_3$ , and *T* isomers compared to fast isomerization of other less thermodynamically stable isomers to  $C_1$ ,  $C_3$ , and *T* mixture. Although the  $T/C_3/C_1$  ratios improve somehow in samples that were prepared at higher temperatures and/or longer reaction times, these 10–30% differences cannot fully explain the observed anomaly. See also: Gakh, A. A.; Tuinman, A. A. *Tetrahedron Lett.* **2001**, *42* (41), 7137–7139.  
 (18) Gerst, M.; Beckhaus, H.-D.; Rüchardt, C.; Campbell, E. E. B.; Tellmann, R. *Tetrahedron Lett.* **1993**, *34* (48), 7729–7732.



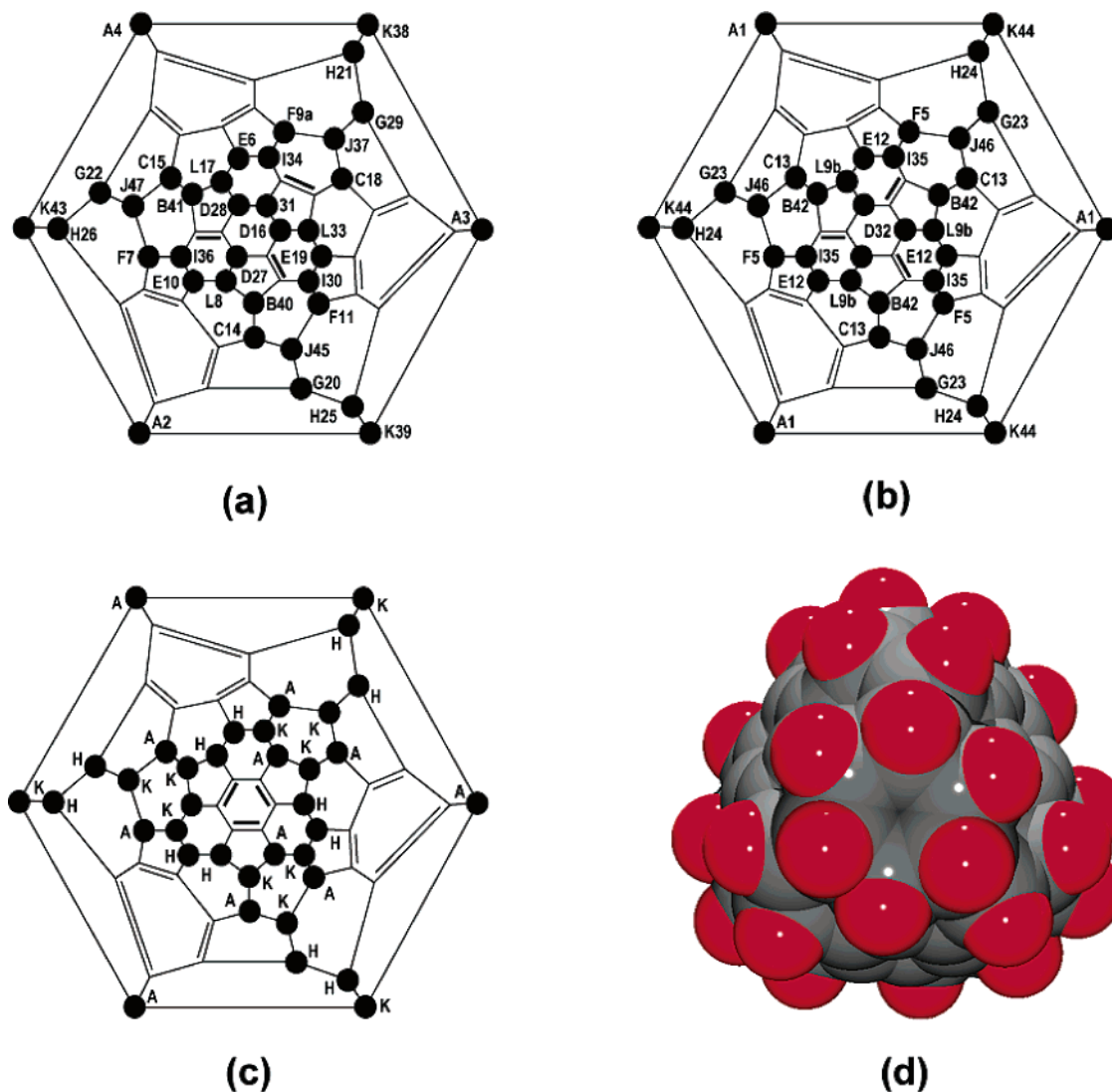


**Figure 4.** The space-filling model (d) and the Shlegel diagrams of  $C_{60}H_{36}$  isomers:  $C_1$  isomer (a),  $C_3$  isomer (b), and  $T$  isomer (c). Each isomer (enantiomer pair) is represented by only one diagram; a full set of six diagrams can be generated by mirror reflection. Isolated double bonds are marked in bold for clarity.

existence of facile hydrogen migration (“hydrogen dance”) on the fullerene surface during high-temperature hydrogenation. Comparison of the structures of the  $C_{60}H_{36}$  isomers with those of the dehydrogenation product provides strong experimental evidence in support of this hypothesis. When  $C_{60}H_{36}$  is subjected to prolonged heating at temperatures above 340 °C in the 9,10-dihydroanthracene melt, it yields a single,  $C_{3v}$  isomer of  $C_{60}H_{18}$  (Scheme 1).<sup>6</sup> The structure of this isomer was established earlier<sup>7</sup> and is incompatible with the structures of both  $C_1$  and  $C_3$ . The  $C_{3v}$  isomer cannot be prepared from either the  $C_1$  or  $C_3$  isomer of  $C_{60}H_{36}$  without rearrangement of existing hydrogens on the fullerene surface (see the Supporting Information). The structure of  $C_{3v}$   $C_{60}H_{18}$  is compatible with the  $T$  isomer of  $C_{60}H_{36}$ , but this isomer cannot be the sole source for  $C_{60}H_{18}$  formation due to its low relative content.

Although the underlying mechanism(s) of facile hydrogen migration on the fullerene surface cannot be unequivocally established at the present time, existing data suggest the hydrogen exchange between 9,10-dihydroanthracene and hydro-[60]fullerenes in the reaction mixtures. It is very likely that the initial hydrogenation leads to a complex “kinetic” mixture of

$C_{60}H_{36}$  isomers which, at elevated temperature, then “anneal” to a mixture consisting of only the most thermodynamically stable isomers. The temperature range of this annealing process is close to the temperature of another process—dehydrogenation<sup>3,19</sup> of  $C_{60}H_{36}$  to  $C_{60}H_{18}$ . The latter compound appears to be the final hydrogenation product at higher temperatures.<sup>6</sup>

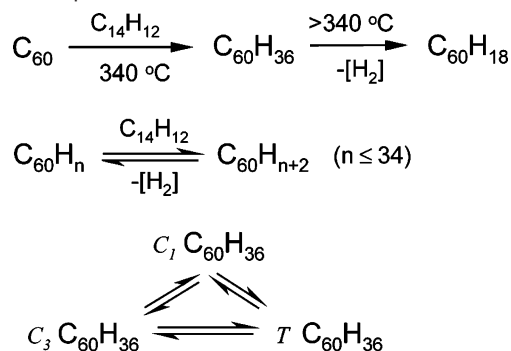
The hypothesis also explains the formation of complex mixtures of  $C_{60}H_{36}$  isomers<sup>5</sup> during Birch reduction of  $C_{60}$  because the reaction conditions do not promote facile hydrogen migration. Taking into consideration the relatively small energy differences between various thermodynamically favored  $C_{60}H_{36}$  isomers,<sup>5,13</sup> it is likely that many of these are being produced.

### Concluding Remarks

An interesting area for future research entails the investigation of hydrogenation patterns in nanocarbon materials that do not contain five-membered rings, such as carbon nanotubes. Although in this case no simple rules can be derived on the basis

(19) Wang, N. X.; Wang, L.; Liu, W.; Ou, Y.; Li, W. *Tetrahedron Lett.* **2001**, 42 (44), 7911–7913.

**Scheme 1.** Hydrogenation/Dehydrogenation<sup>19</sup>/Isomerization Patterns in Fullerene C<sub>60</sub>–9,10-Dihydroanthracene Mixtures at Elevated Temperatures<sup>a</sup>



<sup>a</sup> The actual equilibrium may also include other C<sub>60</sub>H<sub>36</sub> isomers (not shown).

of existing experimental results (such as the three vicinal hydrogens per pentagon rule for C<sub>60</sub>H<sub>36</sub> and related systems), an assumption can be made that hydrogenation of all-hexagon carbon nanostructures would follow certain structural patterns. It is also possible that hydrogenation at elevated temperatures favors facile hydrogen migration, leading to tight surface packing of hydrogen atoms and to production of materials with high mass content of usable hydrogen.

### Experimental Section

**NMR Spectroscopy.** Two-dimensional NMR spectra were recorded at 800 MHz, 20 °C, on saturated solutions of C<sub>60</sub>H<sub>36</sub> in CDCl<sub>3</sub> (approximately 5 mg/mL): a regular inverse [<sup>1</sup>H,<sup>13</sup>C] HSQC spectrum;<sup>20</sup> an inverse COSY-HSQC spectrum with a 20 ms constant-time COSY delay;<sup>10</sup> a TOCSY-HSQC spectrum,<sup>10</sup> recorded with a 18 ms <sup>1</sup>H DIPSI-2 mixing<sup>21</sup> duration using a 10 kHz RF field strength. The HSQC and TOCSY-HSQC spectra were recorded with gradient enhancement.<sup>22</sup> All spectra were recorded with a 10 kHz (49.7 ppm) spectral width in the indirect (<sup>13</sup>C) dimension, and a 5.5 ppm spectral width in the <sup>1</sup>H dimension, using 16 scans and total acquisition times of 12 h (HSQC) and 16 h (COSY-HSQC and TOCSY-HSQC). Acquired data matrices consisted of 800\* × 512\* data points (HSQC) and 1200\* × 512\* data points (COSY-HSQC and TOCSY-HSQC). Time domain data were apodized with 80°-shifted sine bell and squared sine bell windows in the *t*<sub>1</sub> and *t*<sub>2</sub> dimensions, in both cases truncated at 170°. Data matrices

(20) Bodenhausen, G.; Rueben, D. J. *Chem. Phys. Lett.* **1980**, *69*, 185–189.

(21) Shaka, A. J.; Lee, C. J.; Pines, A. J. *Magn. Reson.* **1988**, *77*, 274–293.

(22) Kay, L. E.; Keifer, P.; Saarinen, T. *J. Am. Chem. Soc.* **1992**, *114*, 10663–10665.

were zero-filled to yield a digital resolution of 2.5 Hz (<sup>13</sup>C) and 4.3 Hz (<sup>1</sup>H). Data were processed and analyzed using the NMRPipe software package.<sup>23</sup> One-dimensional NMR spectra were recorded at 400 MHz, 23 °C, on solutions of C<sub>60</sub>H<sub>36</sub> in CS<sub>2</sub>/CDCl<sub>3</sub> (1:1).

**Molecular Calculations.** The geometries and relative thermodynamic characteristics of C<sub>60</sub>H<sub>36</sub> isomers were analyzed using commercially available Chem3D (CambridgeSoft Corporation), Alchemy (Tripos), and HyperChem (Hypercube) computational packages, employing AM1, MM1, MM2, PM3, and 6-31G methods.

**Synthesis of C<sub>1</sub>, C<sub>3</sub>, and T Isomers of C<sub>60</sub>H<sub>36</sub>.** C<sub>60</sub> (200 mg, 0.28 mmol) and 9,10-dihydroanthracene (5.0 g, 28 mmol) were slowly brought to boiling (Wood alloy bath) in a flow of nitrogen. The purple-red mixture was kept for approximately 2 h at 340 ± 10 °C under a slight nitrogen pressure (to prevent excessive boiling of 9,10-dihydroanthracene, bp 312 °C). Progress of the reaction was monitored by TLC (hexane–benzene, hexanes–ethyl acetate). At the end of the reaction excess pressure of nitrogen was released, and the pale yellow reaction mixture was allowed to cool to room temperature. The melt was crushed with a spatula and extracted many times with ether, first by decantation, and then using a Millipore teflon filter. The ether filtrate was periodically checked for the presence of anthracene-derived products by evaporation of a small portion of the solvent and detection of the fluorescence of the residue under a UV lamp. After the disappearance of detectable fluorescence from the filtrate, pale yellow chunks of C<sub>60</sub>H<sub>36</sub> were collected from the filter and dried in vacuo. The compound was dissolved in a minimal quantity of warm benzene, filtered from small amounts of insoluble products, evaporated, and then dried in vacuo to yield 110 mg (0.15 mmol, 52%) of C<sub>60</sub>H<sub>36</sub> as a pale yellowish cream powder. The NMR solutions were filtered before the experiments. The C<sub>60</sub>H<sub>36</sub> samples contained small amounts of benzene even after 12 h of drying in vacuo at elevated temperatures.

**Acknowledgment.** This research was sponsored in part by the IPP program, U.S. Department of Energy, under Contract DE-AC05-00OR22725 with Oak Ridge National Laboratory, managed and operated by UT-Battelle, LLC.

**Supporting Information Available:** Description of the structure elucidation of the C<sub>1</sub>, C<sub>3</sub>, and T isomers; description of compatibility/incompatibility studies of C<sub>3v</sub> C<sub>60</sub>H<sub>18</sub> versus C<sub>1</sub>, C<sub>3</sub>, and T isomers of C<sub>60</sub>H<sub>36</sub>; bibliographic references pertaining to the history of C<sub>60</sub>H<sub>36</sub> research (67 references). This material is available free of charge via the Internet at <http://pubs.acs.org>.

JA035332T

(23) Delaglio, F.; Grzesiek, S.; Vuister, G. W.; Zhu, G.; Pfeifer, J.; Bax, A. J. *Biomol. NMR* **1995**, *6*, 277–293.